Aerosol and Air Quality Research, 18: 1375–1390, 2018

ISSN: 1680-8584 print / 2071-1409 online
doi: 10.4209/aaqr.2017.10.0413

Chemical Characteristics and Source Apportionment by Two Receptor Models of Size-segregated Aerosols in an Emerging Megacity in China

Nan Jiang, Ke Wang*, Xue Yu, Fangcheng Su, Shasha Yin, Qiang Li, Ruiqin Zhang*

Research Institute of Environmental Science, College of Chemistry and Molecular Engineering, Zhengzhou University, Zhengzhou 450001, China

ABSTRACT

$PM_{2.5}$, $PM_{2.5-10}$, and PM_{10} samples were collected in Zhengzhou in 2014 to examine the chemical characteristics and sources of aerosols in this area. The PM concentrations, nine water soluble inorganic ions, organic carbon, elemental carbon, and twenty-two elements were determined, and positive matrix factorization (PMF) and chemical mass balance (CMB) were used for source apportionments. The meteorological impact was also evaluated by back-trajectory cluster analysis. Severe PM pollution was present in the study area, and the aerosol concentrations of $PM_{2.5}$ samples (92%) and PM_{10} samples (85%) significantly exceeded the recommended levels of the Chinese National Ambient Air Quality Standard (NAAQS), with the average annual mass concentrations of $PM_{2.5}$ and PM_{10} reaching 187 and 281 μg m^{-3}, respectively. Secondary inorganic aerosols were the major ions in PM and accounted for 36%, 10%, and 27% of $PM_{2.5}$, $PM_{2.5-10}$, and PM_{10}, respectively. The annual concentration of As (0.029 μg m^{-3}) and Cd (0.010 μg m^{-3}) in PM_{10} also exceeded the Chinese NAAQS levels, indicating a high health risk. Results from source apportionment by PMF modelling indicated that dust, vehicular traffic, coal combustion, secondary aerosols, and industry were the main pollution sources, accounting for 13.1%, 14.1%, 16.1%, 35.8%, and 14.6% of $PM_{2.5}$; 25.1%, 20.8%, 21.8%, 10.5%, and 11.6% of $PM_{2.5-10}$; and 19.8%, 15.8%, 18.5%, 22.5%, and 13.5% of PM_{10}, respectively. Dust sources played an important role in PM pollution, especially coarse particles; however, secondary aerosol sources contributed the most to $PM_{2.5}$. Both of these observations were consistent with the results of mass reconstruction of the size-segregated aerosols. The CMB results coincided with the PMF results for $PM_{2.5}$. Cluster analysis showed that air quality in the study area across the four seasons was mainly affected by air masses from the northeast and the east.

Keywords: Size-segregated; Positive matrix factorization; Chemical mass balance; Back-trajectory clustering analysis.

INTRODUCTION

Through transport and dispersion, air pollution influences climate and weather patterns at relatively large spatial scales (100–1000 km) (Hadley, 2017). Especially, PM pollution has become a common environmental problem in megacities worldwide and is attracting considerable attention in different research fields (Chen *et al.*, 2003; Kang *et al.*, 2004; Sun *et al.*, 2006; Zhang *et al.*, 2013a). This pollution type is closely related to particle constituents and meteorological conditions, and holds important implications for human health, visibility, economy, weather, and the global climate (Charlson *et al.*, 1992; Chameides *et al.*, 1999; Ramanathan *et al.*, 2001). The climatic and health effects of size-segregated aerosols vary considerably because of different particle sizes (Wang *et al.*, 2012). Among the particles, PM_{10} and $PM_{2.5}$ are widely studied.

Understanding of mass concentrations, chemical compositions, and sources is essential to reduce PM pollution. Atmospheric PM is a complex mixture of both primary and secondary particle species, including water-soluble inorganic ions (WSIIs), elements, organic carbon (OC), and elemental carbon (EC). Studying the chemical compositions of PM is important in assessing the effects of PM on air quality and human health and for conducting source apportionment (Tao *et al.*, 2013). Understanding the sources and their contributions to atmospheric PM formation is also important to mitigate air pollution. Mathematical models, together with PM sampling and chemical characterization, have been shown to be extremely useful in order to interpret and understand the geographical distribution, temporal evolution, and origin of pollutants. Receptor models, particularly positive matrix factorization (PMF) and chemical mass balance (CMB), are advanced source apportionment methods for successfully assessing particle source contributions and have been applied in numerous locations worldwide (Xie

* Corresponding author.
E-mail address: dronslayer@126.com (K. Wang); rqz001@163.com; jiangn@zzu.edu.cn (R. Zhang)

et al., 1999; Kim *et al.*, 2003; Gianini *et al.*, 2013; Shi *et al.*, 2014; Manousakas *et al.*, 2015; Contini *et al.*, 2016).

Fig. 1 shows the 2014-based annual average Moderate Resolution Imaging Spectroradiometer Terra Deep Blue aerosol optical depth (AOD) at 550 nm over the entirety of China (a) and Henan Province (b). The data indicate that the aerosol problem in China exhibits distinct regional characteristics, and in terms of AOD, the most deteriorated regions include the North China Plain (including Henan Province), the Yangtze River Delta region, the Pearl River Delta region, and the Sichuan Basin. A similar result was also reported by Luo *et al.* (2014). In brief, most of Henan Province experiences high AOD problems, particularly in Zhengzhou, the capital city of Henan Province.

Several studies have investigated the chemical composition and sources of $PM_{2.5}$ in Zhengzhou, which is predicted by the Economist Intelligence Unit as an emerging megacity in China at around 2020, similar to Beijing, Shanghai, and Guangzhou (Economist Intelligence Unit, 2012). Wang *et al.* (2016b) investigated the WSIIs and carbonaceous components of $PM_{2.5}$ in Zhengzhou from 2011 to 2013. Geng *et al.* (2013) used PMF and determined that soil dust, secondary aerosol, and coal combustion were the $PM_{2.5}$ main sources in 2010. However, given the rapid urbanization and economic development in Zhengzhou, sources of $PM_{2.5}$ possibly varied correspondingly. For example, in 2014, floor space of buildings under construction totaled 1.76×10^8 m^2, the number of civil vehicles reached 1.93 million, and coal consumption by the above designated size industrial enterprises amounted to 35.21 million tons in Zhengzhou (Bureau of Statistics of Henan Province, 2015); these values were much higher than those in 2010 (8.88×10^7 m^2, 0.96 million, and 26.66 million tons, respectively) (Bureau of Statistics of Henan Province, 2011). According to the data from the Ministry of Environmental Protection of the People's Republic of China (MEPPRC, http://www.mep.gov.cn/), Zhengzhou is among the 10 Chinese cities with the poorest air quality in 2014 (MEPPRC, 2015) and featured severe PM pollution. Data from national monitoring sites reveal that $PM_{2.5}$ and PM_{10} are the primary pollutants in Zhengzhou in 2015 and suggest the importance of systematic studies. However, no study has been conducted on chemical compositions and source apportionment of $PM_{2.5}$ in Zhengzhou in 2014, nor compared pollution characteristics and sources of size-segregated aerosols (i.e., $PM_{2.5}$, $PM_{2.5\text{-}10}$, and PM_{10}).

Therefore, in this study, $PM_{2.5}$, $PM_{2.5\text{-}10}$, and PM_{10} samples were collected in an urban area in Zhengzhou through a one-year observation program, and concentrations of PM, WSIIs, OC, EC, and elements were determined. Given the chemical characterization, source apportionment of $PM_{2.5}$, $PM_{2.5\text{-}10}$, and PM_{10} were performed via PMF and CMB. Meteorological impact was also analyzed by back-trajectory cluster analysis. This study is expected to provide fundamental information, including pollution characteristics and sources of PM, for regulatory agencies to mitigate PM pollution in this area.

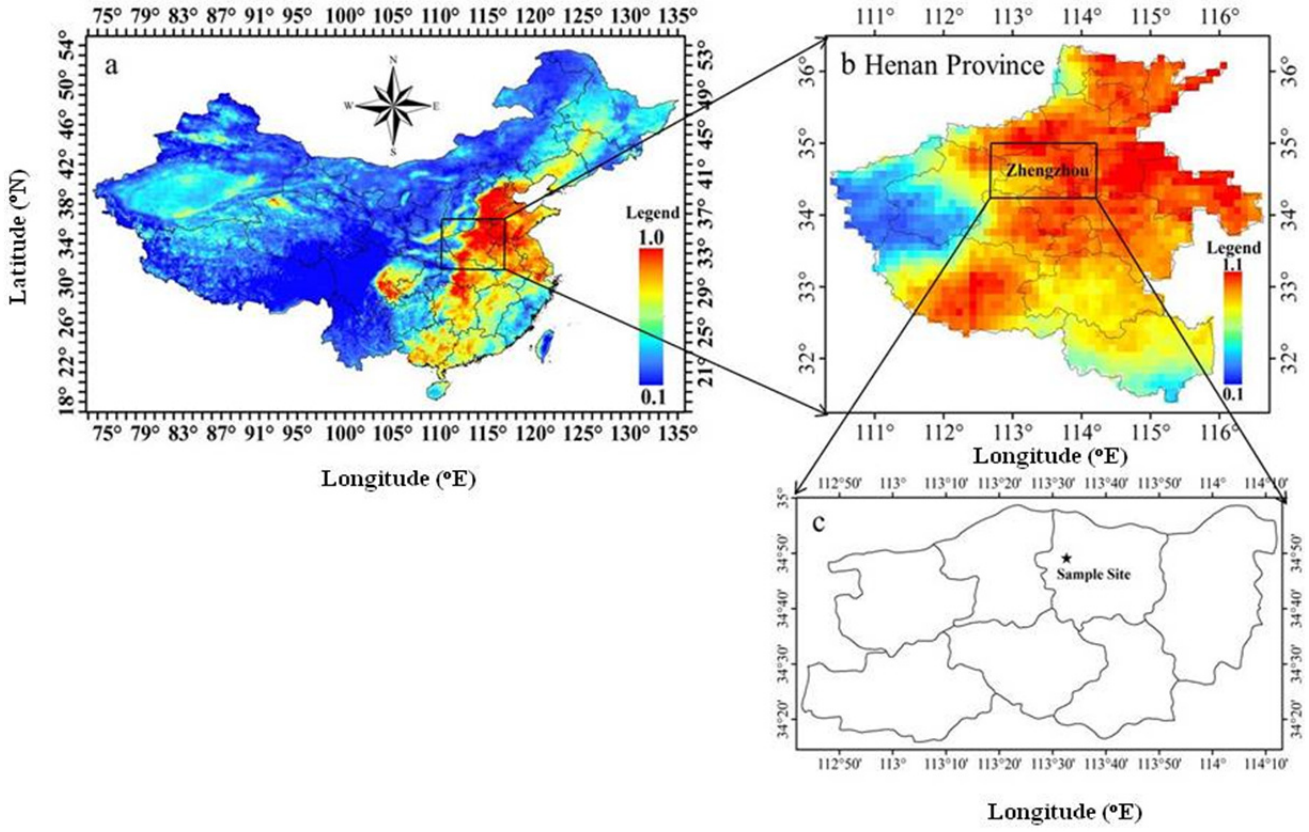

Fig. 1. Location of the sample site (c) and the annual average 10×10 km^2 spatial resolution Terra MODIS Deep Blue AOD at 550 nm over the entirety of China and in Henan Province (a, b) (data from Tao *et al.* (2016)).

EXPERIMENTAL METHODS

Sampling

PM samples were collected between December 2, 2013, and October 24, 2014, at the same sampling site of our previous study in Zhengzhou (Wang *et al.*, 2015). Fig. 1(c) shows the location of sampling site. Sampling was conducted at approximately 9:00 a.m. to 8:00 a.m. of the following day by using two high-volume PM samplers (TE-6070D, Tisch Environmental, USA) at a flow rate of 1.13 m^3 min^{-1}. Sampling was performed during the four seasons, and 12 to 14 samples for each size fraction were collected for each season. Quartz fiber filters (20.3 cm × 25.4 cm, Pall, USA) for $PM_{2.5}$ and PM_{10} were used simultaneously for each sampling. Flow calibration was performed before sampling for each season.

The quartz filters were baked at 450°C for 5 h to remove adsorbed organics. The filters were then placed in a clean room for at least 48 h under constant temperature (25 ± 5°C) and relative humidity (45% ± 5%) before they were weighed using an analytical balance (Mettler Toledo XS205, Switzerland).

Chemical Analysis

Quartz filters were cut into pieces, with each piece featuring an area of 10.9 cm^2. Two filter pieces were used to determine the mass concentrations of WSIIs. Samples were extracted in 25 mL ultrapure water for 30 min in an ultrasonic bath. Four anions (F^-, Cl^-, NO_3^-, and SO_4^{2-}) and five cations (Na^+, NH_4^+, K^+, Mg^{2+}, and Ca^{2+}) were analyzed by ion chromatography (ICS-90, Dionex, USA). Additional details were described by Wang *et al.* (2016b).

OC and EC concentrations were determined through thermal/optical transmittance method (Chow *et al.*, 2001) by using a carbon analyzer (Model 5L, Sunset Laboratory, USA). Further information was described in our previous studies (Geng *et al.*, 2013; Wang *et al.*, 2016b).

Six pieces of filters (10.9 cm^2 each) were placed in a digestion cell (polytetrafluoroethylene) with a mixture of acids (11.1% HNO_3/33.5% HCl). The digestion cell was then placed in a microwave digestion instrument (ETHOS ONE, MILE STONE, Italy). Digestion occurred under high-pressure with advantages of low dosage of reagents, which were digested almost completely. After cooling and filtering, 22 elements, including Be, Mg, Al, Ti, Mo, Mn, Fe, Co, Ni, Cu, Zn, V, Se, As, Sr, Ag, Cd, Sn, Sb, Ba, Tl, and Pb, were analyzed in the present study via inductively coupled plasma-mass spectrometry (Agilent7500cx, Santa Clara, CA, USA).

Quality Assurance and Quality Control

Field blank filters were measured as blank concentrations. According to US Environmental Protection Agency (EPA) (2016), standard deviation of replicate instrumental measurements of spiked blanks was used to calculate the method detection limit (MDL). For chemical analysis, each filter was measured twice, with errors considered acceptable within 5%.

For WSIIs, field blank concentrations ranged from 0.00 μg m^{-3} (F^-) to 0.03 μg m^{-3} (Ca^{2+}). External standard method was used for quantification. Coefficient of determination (R^2) of the calibration curves were over 0.9996 for all observed ions, except NH_4^+ (0.9988). The MDLs of Na^+, NH_4^+, K^+, Mg^{2+}, Ca^{2+}, F^-, Cl^-, NO_3^-, and SO_4^{2-} reached 0.12, 0.02, 0.04, 0.01, 0.04, 0.07, 0.11, 0.13, and 0.17 μg mL^{-1}, respectively. For the recovery test, standard addition recovery of the nine ions ranged between 89% and 110%.

For OC and EC, the analyzer was calibrated via a sucrose standard solution before measurement. Field blank concentrations measured 0.5 and 0.0 μg m^{-3} for OC and EC, respectively. MDL amounted 0.2 μg cm^{-2} for OC and EC.

For the elements, standard recovery efficiencies were determined, with values ranging from 80% to 120%. MDLs were calculated and ranged from 0.002 ng m^{-3} (Ag) to 3.362 ng m^{-3} (Sb). R^2 values of the standard curve for the 22 trace elements studied were all higher than 0.9989.

PMF and CMB Models

PMF 5.0 and CMB 8.2 models, as recommended by the US EPA, were both used in this study for source apportionment of atmospheric PM. Intercomparisons of PMF and CMB were conducted for mutual validation of the two model outputs given the unknown overall uncertainty of the applied models (Gianini *et al.*, 2013). By contrast, CMB requires a specified priori information of emission sources and their profiles; however, PMF only necessitates qualitative or semi-quantitative a posteriori information of source emission profiles (Gianini *et al.*, 2013).

PMF is a convenient factor analysis model (Paatero and Tapper, 1994) based on the weighted least square fit approach. Input data include concentrations and uncertainties of all species. The sample data matrix was decomposed into factor contribution matrix and factor profile matrix by PMF. For species concentrations, as data pretreatment, missing data and values below MDL were replaced by the species median and 0.5 × MDL, respectively (Brown *et al.*, 2015; Cesari *et al.*, 2016a; Jiang *et al.*, 2018c). For uncertainties, the values considered were 0.1 × concentration + MDL/3 (species concentration > MDL), 0.2 × concentration + MDL/3 (species concentration < MDL), or four times the species-specific median (missing data) (Tauler *et al.*, 2009; Jang *et al.*, 2013). According to the US EPA (2014), bootstrap (BS) was run with 100 resamples, which is the recommended value of the model, and results were considered acceptable with all factors for PM in PMF analysis mapping above 80% of the BS runs; to determine a more optimal solution, Fpeak was conducted with strengths between –3 and 3; variations in G-space plots, profiles, and contributions were compared for solution optimization. We also adopted the constrained model to optimize the solution. When all parameters meet the performance requirements of PMF, i.e., intercept ~0, slope ~1, $R^2 > 0.6$, and signal-to-noise ratio and residuals for reliable model run are appropriate, results of source apportionment are considered acceptable (US EPA, 2014). Other details, including species categorization, are described by the US EPA (2014), Cesari *et al.* (2016b), and Wang *et al.* (2017).

CMB requires ambient data and source profiles as inputs to estimate and quantify source contributions, on the basis of effective variance-weighted least squares fitting. Missing data (i.e., invalid) are automatically removed from calculation, and concentrations below MDL are also replaced by 0.5 × MDL (US EPA, 2004; Yatkin and Bayram, 2008). Performance of CMB result is controlled by four diagnostic parameters, and when all parameter values meet the requirements of CMB, i.e., T-statistics > 2.0, coefficient of determination > 0.8, Chi-square < 2, and 80% < percent mass < 120%, source apportionment results are considered acceptable (US EPA, 2004).

Back-trajectory Cluster Analysis

The Hybrid Single Particle Lagrangian Integrated Trajectory Model (HYSPLIT) is a powerful tool for studying long-range transport route of air masses. In this study, HYSPLIT_4 transport model was applied to assess the potential influences of regional transport and PM compositions, which vary widely under the prevailing wind, in four seasons. The 24-h backward wind trajectories at 500 m above ground level above the monitoring site (34°48′N, 113°31′E) were calculated with each campaign day including four backward trajectories. Then, on the basis of the similarity in spatial distribution, trajectories were clustered, and the suitable cluster number was selected before the dramatic increase in total spatial variation percentage (Wang, 2014).

RESULTS AND DISCUSSION

General Characterization

Major Precursors and Meteorological Variables

Table 1 lists the major precursors of PM (data from the national monitoring site) and meteorological variables in the study area. Wind speeds measured between 0.5 m s^{-1} to 4.5 m s^{-1}, and annual average value of 1.9 ± 0.7 m s^{-1} was half of that in Shanghai (2011–2013: 3.9–4.2 m s^{-1}; Wang *et al.*, 2016a). The low wind speed was the disadvantage of contaminant dispersion. Mean ambient temperature was the highest in summer (28.1 ± 1.9°C) and lowest in winter (4.3 ± 3.4°C). Annual average value of relative humidity reached 57% ± 14%. The major precursors of PM, i.e., SO_2, NO, and NO_2 (Krotkov *et al.*, 2016; Jiang *et al.*, 2017), showed notable seasonal variations, with the highest concentrations in winter (142 ± 55, 105 ± 46, and 87 ± 17 μg m^{-3}, respectively), and the lowest in summer (24 ± 9, 7 ± 3, and 46 ± 8 μg m^{-3}, respectively). During winter, enhanced emission of coal consumption for central heating, subsidence of the atmospheric mixing layer, and the prevailing stable atmospheric conditions (Zheng *et al.*, 2015) resulted in high-level pollution. Daily NO_2 and SO_2 concentrations varied from 29 μg m^{-3} to 108 μg m^{-3} and from 17 μg m^{-3} to 244 μg m^{-3}, with approximately 29% and 8% of sampling days exceeding the Chinese National Ambient Air Quality Standard (NAAQS) (daily standard: 80 and 150 μg m^{-3} for NO_2 and SO_2, respectively). Annual values of NO_2 and SO_2 were 68 ± 20 and 63 ± 52 μg m^{-3}, respectively, which exceed the NAAQS values (annual standard: 40 and 60 μg m^{-3} for NO_2 and SO_2, respectively), especially for NO_2. High precursor levels possibly play an important role in PM pollution.

$PM_{2.5}$, $PM_{2.5\text{-}10}$, and PM_{10} Mass Concentrations

Fig. 2 displays the daily PM concentrations during the sampling period. $PM_{2.5\text{-}10}$ concentrations were separately calculated from PM_{10} and $PM_{2.5}$. Concentrations of $PM_{2.5}$, $PM_{2.5\text{-}10}$, and PM_{10} lay in the ranges of 68–698 μg m^{-3}, 18–257 μg m^{-3}, and 109–918 μg m^{-3}, with annual averages of 187 ± 134, 94 ± 44, and 281 ± 171 μg m^{-3}, respectively. Approximately 92% of $PM_{2.5}$ samples and 85% of PM_{10} samples exceed the Chinese NAAQS values (daily standard: 75 and 150 μg m^{-3}, respectively). Annual average concentrations were much higher than those of the Chinese NAAQS (annual standards: 35 μg m^{-3} ($PM_{2.5}$) and 70 μg m^{-3} (PM_{10})). These findings held especially true for the $PM_{2.5}$ level, which was 4.3 times higher than the standard. Comparison was conducted to fully comprehend PM pollution levels in the study site. Levels of $PM_{2.5}$ and PM_{10} in the study area were respectively higher than those in Beijing (102 and 149 μg m^{-3}) (Guo *et al.*, 2010), Shanghai (103 and 149 μg m^{-3}) (Wang *et al.*, 2013), Tangshan (79 and 151 μg m^{-3}) (Zhou *et al.*, 2011), and Guangzhou (2006: 61 and 93 μg m^{-3}; 2009: 45 and 75 μg m^{-3}) (Peng *et al.*, 2011). The PM concentrations measured in the study area were one or two orders of magnitude higher than the annual average values in 42 sites in the US (2–15 μg m^{-3} for $PM_{2.5}$ and 4–21 μg m^{-3} for PM_{10}) (Eldred *et al.*, 1997) and Europe (8–40 μg m^{-3} for $PM_{2.5}$ and 19–53 μg m^{-3} for PM_{10}) (Querol *et al.*, 2004); these observations suggest the presence of severe PM pollution in the study area. $PM_{2.5}/PM_{10}$ ratios in the study area ranged from 0.50 to 0.90, and annual ratio was 0.65, similar to those in Shanghai (two sites: 62% and 68%) (Wang *et al.*, 2013) and slightly lower than that in Hangzhou (0.70) (Bao *et al.*, 2010). These findings imply that fine particles represent the main mass in PM_{10}.

Table 1. Major precursors and meteorological variables during the sampling period.

	Wind speed (m s^{-1})	Relative humidity (%)	Ambient temperature (°C)	SO_2 (μg m^{-3})	NO (μg m^{-3})	NO_2 (μg m^{-3})
Winter	1.4 ± 0.6	52 ± 14	4.3 ± 3.4	142 ± 55	105 ± 46	87 ± 17
Spring	2.1 ± 0.5	52 ± 14	18.6 ± 2.0	50 ± 25	16 ± 10	71 ± 15
Summer	2.2 ± 0.6	62 ± 5	28.1 ± 1.9	24 ± 9	7 ± 3	46 ± 8
Autumn	1.7 ± 0.9	62 ± 17	18.0 ± 1.3	52 ± 21	22 ± 13	73 ± 11
Annual	1.9 ± 0.7	57 ± 14	18.0 ± 8.5	63 ± 52	34 ± 44	68 ± 20

Hourly concentration data of SO_2, NO and NO_2 are from the national monitoring site.

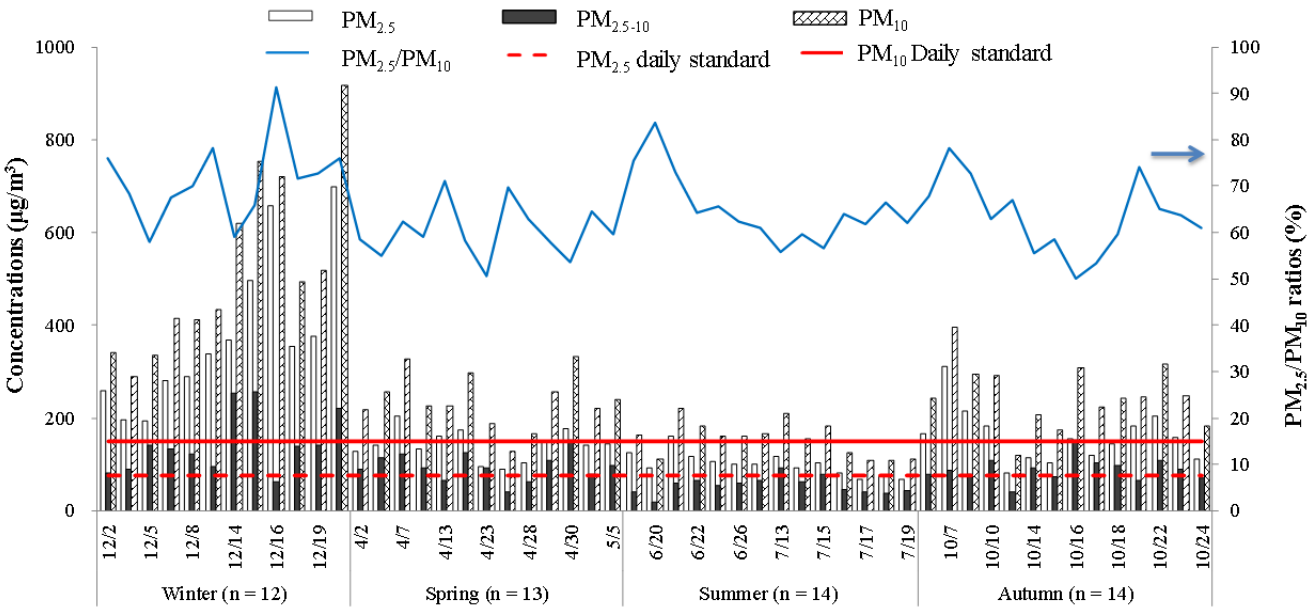

Fig. 2. $PM_{2.5}$, $PM_{2.5\text{-}10}$, and PM_{10} daily mass concentrations during the sampling period.

Main WSIIs and Carbon

Fig. 3 and Table S1 in the Supplemental Materials provide the mean values of PM mass concentrations, WSIIs content, OC, and EC. Average concentrations of $PM_{2.5}$, $PM_{2.5\text{-}10}$, and PM_{10} showed remarkable seasonal characteristics, i.e., winter (376, 149, and 524 μg m^{-3}) > autumn (160, 89, and 249 μg m^{-3}) > spring (136, 90, and 226 μg m^{-3}) > summer (100, 54, and 155 μg m^{-3}). These results were attributed to the comprehensive influence of various meteorological conditions and source emissions. In winter, frequent stagnant atmospheric condition and extra coal consumption for domestic heating lead to the highest PM concentrations, which can be demonstrated by the high levels of SO_4^{2-}, OC, Cl^-, and EC in this season. Secondary inorganic aerosols (SIAs), including SO_4^{2-}, NO_3^-, and NH_4^+, were the major ions in PM, and accounted for 36%, 10%, and 27% of $PM_{2.5}$, $PM_{2.5\text{-}10}$, and PM_{10}, respectively. This finding suggested that SIAs were mainly present in fine particles, as reported by previous studies (Kong *et al.*, 2010; Long *et al.*, 2014). The ratios of Ca^{2+}, Mg^{2+}, and F^- in $PM_{2.5}$ and $PM_{2.5\text{-}10}$ were relatively comparable and featured small gaps. Correlation coefficients should be evaluated to identify similar sources of atmospheric particulates. As shown in Table S2 in the Supplemental Materials, Spearman correlation coefficients among WSIIs in $PM_{2.5}$, $PM_{2.5\text{-}10}$, and PM_{10} were determined via IBM SPSS for Windows, Version 21.0. The ions possibly originated from the same source when correlation coefficients were close to 1. NO_3^- and SO_4^{2-} exhibited good correlations with NH_4^+ (R^2 = 0.87 and 0.88 in $PM_{2.5}$, R^2 = 0.44 and 0.71 in $PM_{2.5\text{-}10}$, R^2 = 0.87 and 0.86 in PM_{10}, respectively), suggesting the presence of NH_4NO_3 and $(NH_4)_2SO_4$. Cl^- exhibited a high correlation with K^+, thereby indicating that PM pollution could be affected by biomass burning (Silva *et al.*, 1999). Ca^{2+} and Mg^{2+} are marker elements of crust matter (Winchester *et al.*, 1979) and reflect the valuable contributions of dust sources.

Elemental Concentration

Fig. 4, Tables S3 and S4 in the Supplemental Materials show the mean concentrations and size distributions of trace element in $PM_{2.5}$, $PM_{2.5\text{-}10}$, and PM_{10}. Total elemental concentrations accounted for approximately 3.5% of PM and exhibited the same seasonal characteristics as the PM level, i.e., they were highest in winter and lowest in summer. For $PM_{2.5}$, Al and Fe, with concentrations exceeding 1000 ng m^{-3}, accounted for 58% of total elements, whereas Zn, Mg, and Pb in fine particles, with concentrations between 100 and 1000 ng m^{-3}, accounted for 34%. With concentrations less than 100 ng m^{-3}, the remaining 17 elements in $PM_{2.5}$, i.e., Mn, Ba, Ti, Cu, Sr, As, Sn, Cd, Sb, Se, Ni, Mo, V, Tl, Ag, Co, and Be, accounted for 8% of the total elements. Similarly, for PM_{10}, Al and Fe accounted for 65% of the total elements; Zn, Mg, Pb, Mn, Ti, and Ba accounted for 27%; the remaining 14 elements accounted for 8%. Annual concentration of As (0.029 μg m^{-3}) and Cd (0.010 μg m^{-3}) in PM_{10} significantly exceeded the Chinese NAAQS (0.006 and 0.005 μg m^{-3} for As and Cd, respectively, in atmospheric environment including both gas and particle phase), with a relative high health risk. For different size distributions, Zn, Pb, Mn, Cu, As, Sn, Cd, Sb, Se, Ni, Mo, Tl, and Ag mainly fell under $PM_{2.5}$, with ratios between 67% (Mo) and 96% (Se). However, Al, Fe, Mg, Ti, Ba, Sr, V, Co, and Be were relatively comparable under $PM_{2.5}$ and $PM_{2.5\text{-}10}$, especially Ba and Sr, which exhibited a higher ratio in $PM_{2.5\text{-}10}$ than in $PM_{2.5}$. In a previous study, Al, Fe, and Mg were reported to be crust elements mainly originating from dust emission (Winchester *et al.*, 1979); this observation indicates that high PM level in this study area is influenced by dust. Zn, Pb, and Mn are closely related to vehicle brake, wear, and fuel combustion emissions (Garg *et al.*, 2000; Cheng *et al.*, 2010; Lin *et al.*, 2014), whereas Ba, Cd, Cu, Sb, Sn, and Mo are emitted from tire tread and brake lining wear (Garg *et al.*, 2000;

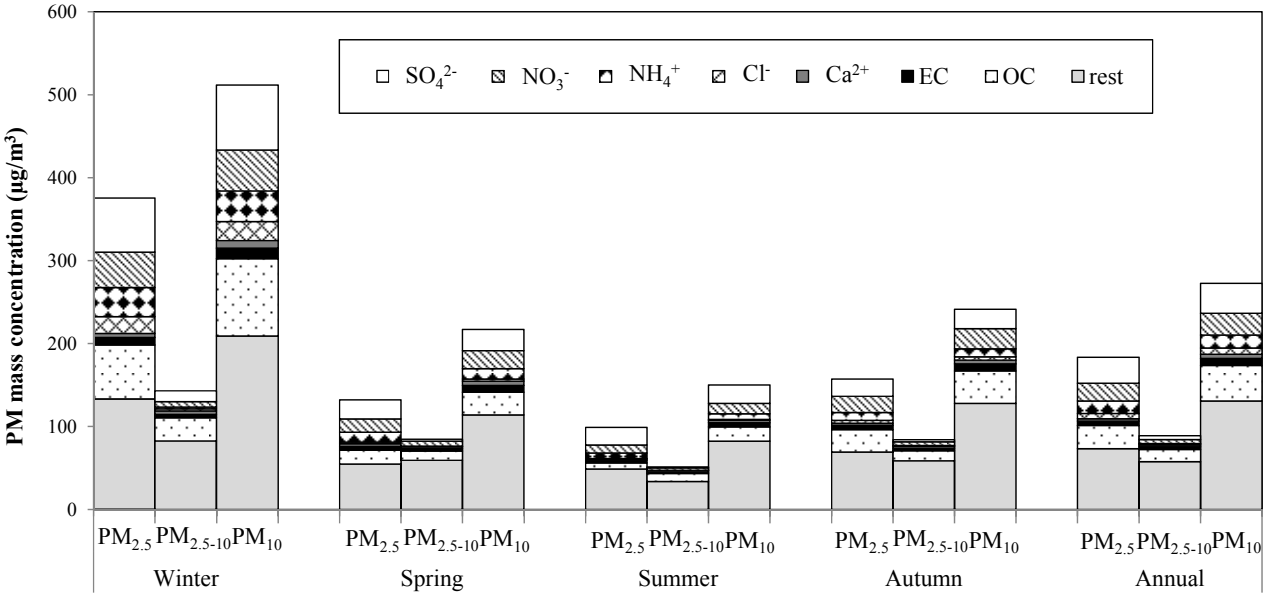

Fig. 3. Mean values of $PM_{2.5}$, $PM_{2.5-10}$ and PM_{10} mass concentration and the main species. rest: the rest of PM except the species shown.

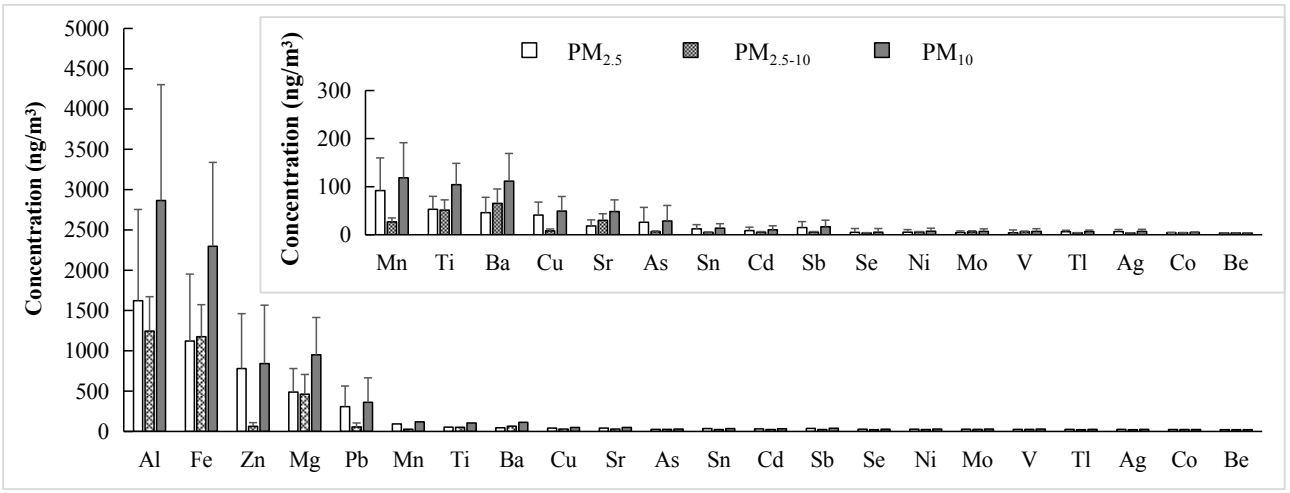

The inserted graph is the enlargement of elements with relative low concentrations.
(a) Annual mean concentrations

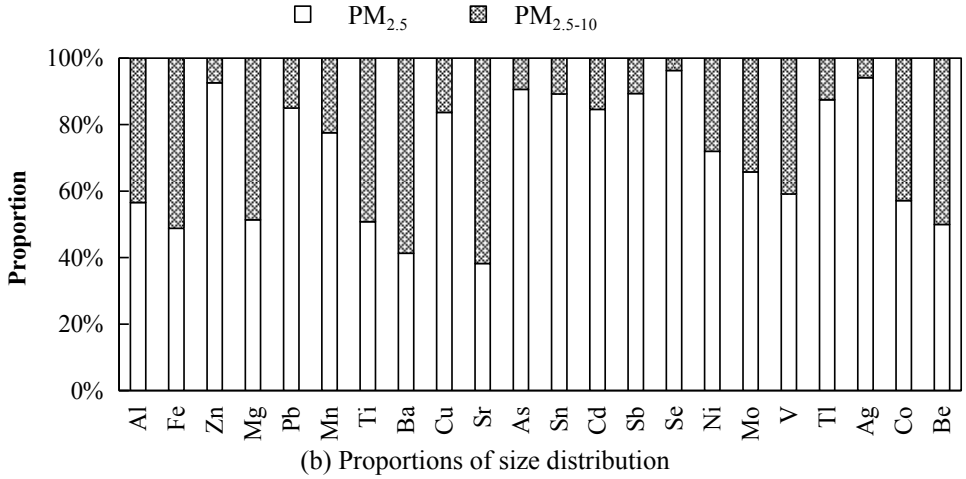

(b) Proportions of size distribution

Fig. 4. Annual mean concentrations (a) and size distribution (b) of trace element of size-segregated aerosols.

Bozlaker *et al.*, 2013; Lin *et al.*, 2014), demonstrating that high PM concentration in this area is affected by vehicles.

Mass Reconstruction of $PM_{2.5}$, $PM_{2.5-10}$, and PM_{10}

In our study, major PM components comprised SIAs, organic mass (OM), EC, and crustal minerals (CM, i.e., Al, Si, Ca, Fe, and Ti). Fig. 5 illustrates the mass reconstruction of the chemical compositions of PM. OM is estimated as OC multiplied by 1.8 (Hand *et al.*, 2011; Simon *et al.*, 2011), and dust mass is calculated as follows (Malm *et al.*, 1994):

$$CM = 2.20 \times [Al] + 2.49 \times [Si] + 1.63 \times [Ca] + 2.42 \times [Fe] + 1.94 \times [Ti] \quad (1)$$

where Si was estimated on the basis of Al-to-Si ratio (0.46) (Chow *et al.*, 2015) in $PM_{2.5}$ and Al-to-Si ratio (0.26) (Taylor and Mclennan, 1995) in $PM_{2.5-10}$ and PM_{10}. CM was calculated using Ca^{2+} concentrations given the lack of values for Ca.

OM, SIAs, and CM were the most abundant species in PM, and accounted for 24%, 36%, and 12% of $PM_{2.5}$; 27%, 10%, and 26% of $PM_{2.5-10}$; and 25%, 27%, and 19% of PM_{10}, respectively. By comparing size-segregated aerosols, CM was more abundant in coarse particles ($PM_{2.5-10}$) than in other particle types. This finding indicates that appropriate measures for dust control are more effective in decreasing PM_{10} level than $PM_{2.5}$ level. However, SIAs mainly exist in $PM_{2.5}$, suggesting that control measures of precursor gases (i.e., SO_2, NO_x, NH_3, and VOCs) may be more successful in mitigating fine particle ($PM_{2.5}$) pollution than coarse particle pollution. Although EC and other elements only approximately accounted for 3% and 1% in PM, these components, especially heavy metals (As, Cu, Zn, Pb, Cd, Cr, and Ni), must still be paid further attention given their environmental and health effects (Martuzevicius *et al.*, 2011; Liu *et al.*, 2015).

Comparison of Source Appointment by PMF and CMB

Four scatter plots of $PM_{2.5}$ and PM_{10} are shown in Fig. S1 in the Supplemental Materials. R^2 ranged from 0.79 to 0.90, indicating similar sources. In this study, PMF 5.0 was used to identify and quantify potential sources of $PM_{2.5}$, $PM_{2.5-10}$, and PM_{10}, and 27 species concentrations and uncertainty of 159 PM samples (53 samples for each size fraction) were used as input data for the model. On the basis of the requirement of analysis input data of PMF 5.0 (US EPA, 2014), the species were classified as "strong," "weak," and "bad" variables. "Weak" variables triple the uncertainty, whereas "bad" variables are excluded from analysis. Additional details are shown in Table 2. To obtain a further realistic solution of iterations and decreased rotational ambiguity (Amato *et al.*, 2016), we applied different constraints to the PMF model during source appointment of size-segregated aerosols, with the dQ values satisfying the requirement of PMF 5.0 (US EPA, 2014); additional details and other parameters (Q_{robust}/Q_{true}, slope, and R^2) are provided in Table 2. Comprehensively considering the

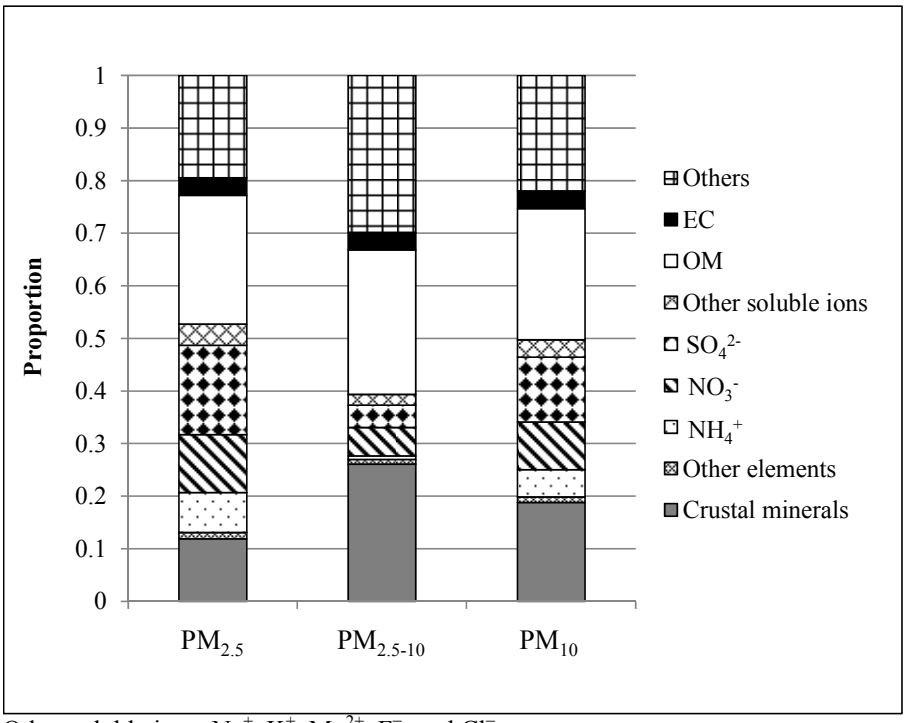

Other soluble ions: Na^+, K^+, Mg^{2+}, F^-, and Cl^-.
Other elements: measured elements except Al, Fe and Ti.
Crustal minerals: Al, Si, Ca (Ca^{2+}), Fe, and Ti.
Others: the rest of PM except the species shown.

Fig. 5. Mass reconstruction of the chemical compositions of $PM_{2.5}$, $PM_{2.5-10}$, and PM_{10}.

Table 2. Summary of input species, constraints and parameters for $PM_{2.5}$, $PM_{2.5\text{-}10}$ and PM_{10} by PMF.

	Input species	Constraints	Parameters
$PM_{2.5}$	**Strong**: EC, OC, Na^+, NH_4^+, K^+, Cl^-, NO_3^-, SO_4^{2-}, Ca^{2+}, Mg, Al, Ti, Mn, Fe, Ni, Zn, As, Ag, Cd, Ba, Tl, Pb, Si **Weak**: Cu, Se **Bad**: V, Sr	– Pulling down the NH_4^+, NO_3^- and SO_4^{2-} contributions in the industrial source profile; – Pulling down the NH_4^+ and SO_4^{2-} contributions in the vehicular traffic source profile	Q_{robust}/Q_{true} = 0.92 Slope = 0.88 R^2 = 0.91
$PM_{2.5\text{-}10}$	**Strong**: OC, Na^+, NH_4^+, K^+, Cl^-, NO_3^-, SO_4^{2-}, Mg, Al, Ti, Mn, Fe, Ni, Cu, Zn, As, Ag, Cd, Pb, Si **Weak**: EC, Ca^{2+} **Bad**: V, Se Sr, Ba, Tl	– Pulling down the Mg and Al contributions in the coal combustion source profile and the Cd and Pb contributions in the secondary aerosol source profile; – Pulling up the NH_4^+, NO_3^- and SO_4^{2-} contributions in the secondary aerosol source profile; – Setting to zero the presence of K^+ and Cl^- in the secondary aerosol factor	Q_{robust}/Q_{true} = 0.92 Slope = 0.81 R^2 = 0.84
PM_{10}	**Strong**: EC, OC, Na^+, NH_4^+, K^+, Cl^-, NO_3^-, SO_4^{2-}, Mg, Al, Ti, V, Mn, Fe, Ni, Cu, Zn, As, Se, Ag, Cd, Ba, Pb, Si **Weak**: Ca^{2+} **Bad**: Sr, Tl	– Pulling up the As, EC and OC contributions in the coal combustion source profile; – Setting to zero the presence of K^+ in the industrial factor; K^+ and As in the secondary aerosol factor; NH_4^+ in the vehicular traffic factor and NH_4^+ in the others factor	Q_{robust}/Q_{true} = 0.83 Slope = 0.86 R^2 = 0.88

Q_{robust}/Q_{true}: a measure of the impact of data points with high scaled residuals.
Slope and R^2: evaluate how well each species is fit for the model; calculated using the observed and predicted data.

distributions of scaled residuals, solution stability, and physically reasonable solutions, the resulting six factors are the optimal choice in the three size fractions. The combination of displacement (DISP), BS, and BS-DISP were conducted to evaluate random errors and rotational ambiguity, and results showed that no swaps were diagnosed for dQ_{max} of 4 and 8; bootstrapped factors were also mapped to base factors over 80%, conforming to the requirement of PMF 5.0 (US EPA, 2014). To obtain a further optimal solution, rotations with an Fpeak value from –3 to 3 were adopted, and the nonrotated solution (Fpeak = 0.0) was selected as the rotated results showed significantly increased Q values, and non-optimizing results, including those of G-space plots, profiles, and contributions, appeared as expected. Fig. 6 presents the PMF results.

Dust was the first factor, and it is characterized by Ca/Ca^{2+}, Mg, Al, Fe, Ti, Mn, Pb, and Si (Lough *et al.*, 2005; Wang *et al.*, 2016c); dust was mixed with EC because of the effect of road dust (Jiang *et al.*, 2018a). Dust source accounted for 13.1%, 25.1%, and 19.8% of $PM_{2.5}$, $PM_{2.5\text{-}10}$, and PM_{10} masses in the study area, respectively (Table 3). Contribution values are consistent with the results of mass reconstructions, revealing that dust source plays an important role in PM pollution, especially in coarse particles, similar to a previous study (Lasun *et al.*, 2016).

The second factor is vehicular traffic, which is mixed with road dust. Vehicular traffic source is characterized by high loads of EC, OC, NO_3^-, Fe, Zn, Cu, and Ni (Viana *et al.*, 2006; Charlesworth *et al.*, 2011). For example, Cu is linked to brake abrasion, whereas Ni is generated from oil combustion (Garg *et al.*, 2000). EC is mainly emitted by heavy-duty vehicles (Manousakas *et al.*, 2015). In this source, the relative high EC content was attributed to site location, which lies close to the west side of 4th Beltway in Zhengzhou, where a considerable quantity of heavy-duty diesel trucks pass. This source contributed 14.1%, 20.8%, and 15.8% to $PM_{2.5}$, $PM_{2.5\text{-}10}$, and PM_{10} in the study area, respectively. This source should be paid additional attention to alleviate PM levels caused by the rising number of vehicles in this area.

The third factor is coal combustion, with high loadings of Cl^-, OC, Na^+, SO_4^{2-}, As, and Pd, which are closely related to this source (Bhangare *et al.*, 2011). Coal combustion is a major PM source and accounted for 16.1%, 21.8%, and 18.5% of $PM_{2.5}$, $PM_{2.5\text{-}10}$, and PM_{10} mass, respectively, with slightly higher contributions in coarse particles, as similarly reported in a previous study (Tian *et al.*, 2016). In previous works, coal combustion has been identified as a highly valuable PM source in China (e.g., coal combustions accounted for 12.4% and 10.5% of $PM_{2.5}$ at two sites in Nanjing in 2013 and 18% of $PM_{2.5}$ in Taian in 2014 [Li *et al.*, 2016; Liu *et al.*, 2016]). According to the China Statistical Yearbook (National Bureau of Statistics of China, 2015), total energy consumption in Henan in 2014 reached 228.9 million tons of standard coal equivalents, with a percentage of 77.7% for coal consumption; this value was much higher than the average proportion in China (64.0%). The energy structure of Henan heavily depends on coal, and this area may face serious PM pollution caused by long-term coal combustion.

The fourth factor is secondary aerosols, which feature high contents of SO_4^{2-}, NH_4^+, and NO_3^-. This source accounted for 35.8%, 10.5%, and 22.5% of $PM_{2.5}$, $PM_{2.5\text{-}10}$, and PM_{10} mass, respectively. Secondary aerosols represent the most important source of $PM_{2.5}$ and PM_{10}, and this

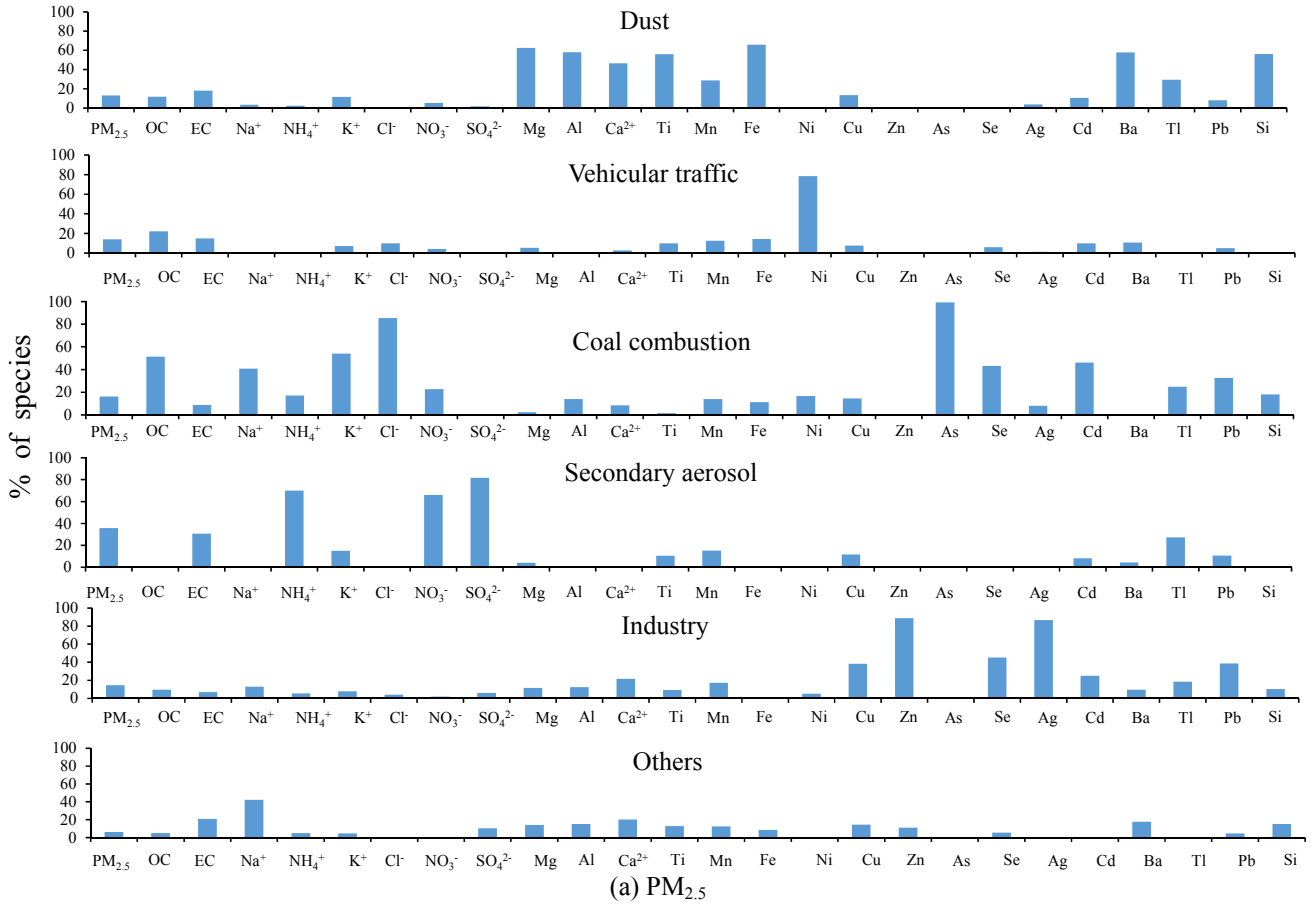

(a) $PM_{2.5}$

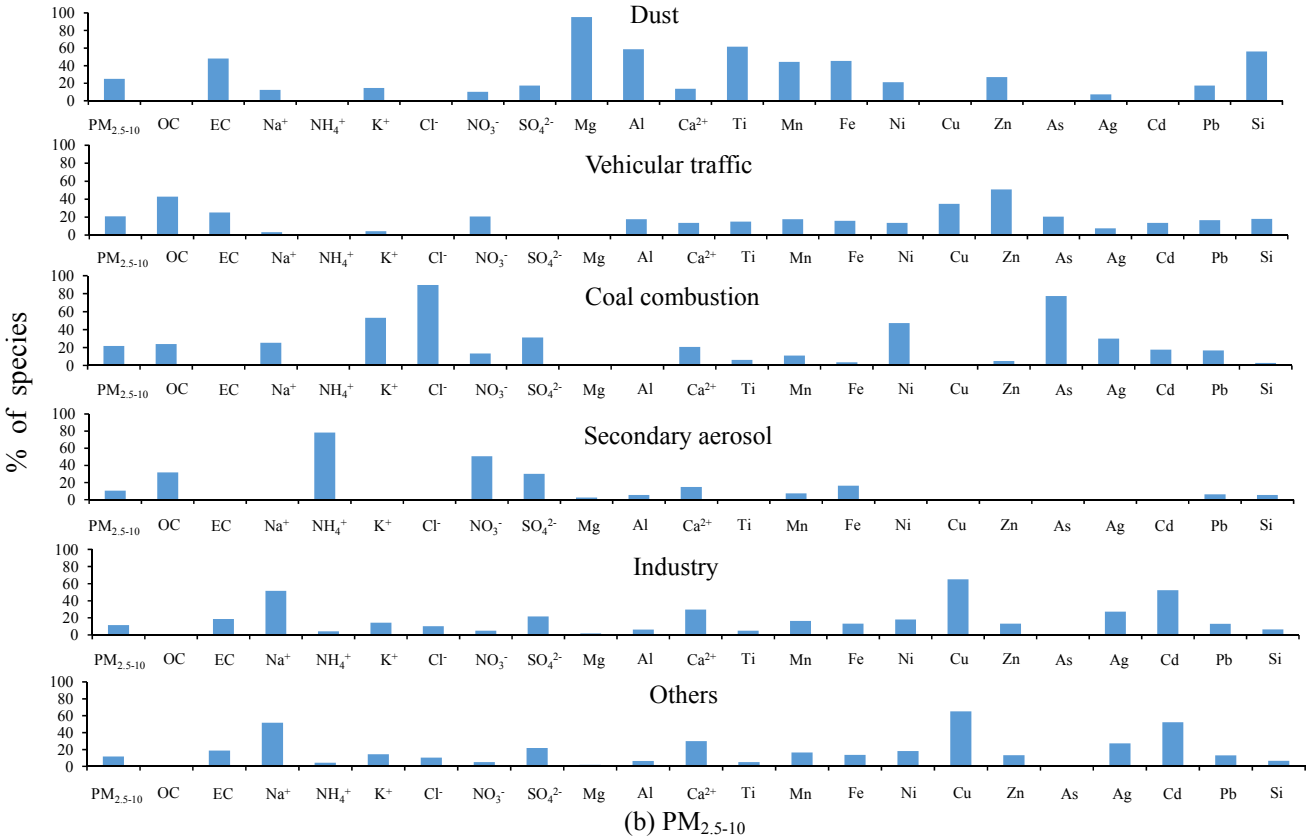

(b) $PM_{2.5\text{-}10}$

Fig. 6. Source profiles of $PM_{2.5}$, $PM_{2.5\text{-}10}$, and PM_{10} obtained by PMF model analysis.

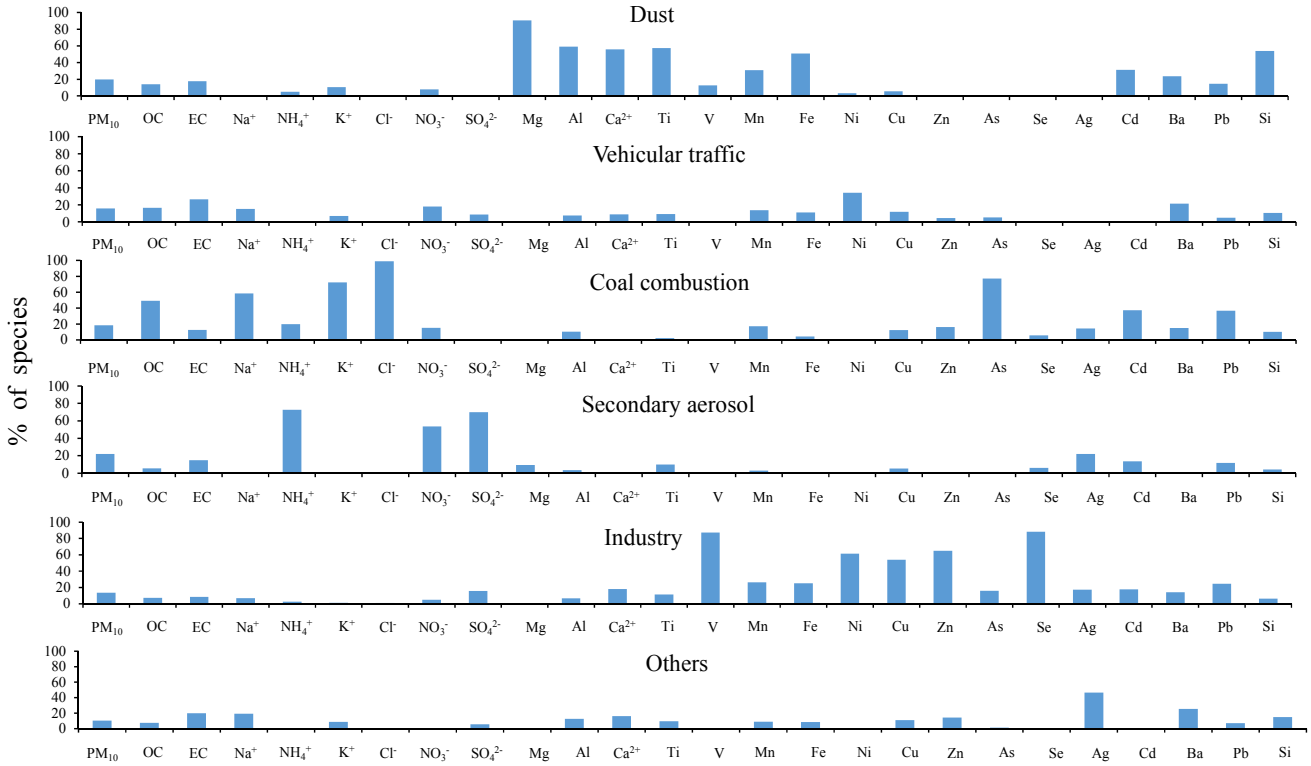

(c) PM_{10}

Fig. 6. (*continued*).

Table 3. Comparison of source contributions (%) to PM by PMF and CMB models.

Sources	$PM_{2.5}$		$PM_{2.5-10}$	PM_{10}
	PMF	CMB	PMF	PMF
Dust	13.1	12.7	25.1	19.8
Coal combustion	16.1	18.8	21.8	18.5
Secondary aerosols	35.8	29.8	10.5	22.5
Vehicular traffic	14.1	11.8	20.8	15.8
Industry	14.6	11.5	11.6	13.5
Biomass burning	-	8.8	-	-
Others	6.3	6.5	11.6	10.3

notion is consistent with the results of mass reconstruction. Contribution value in $PM_{2.5}$ was much higher than that in $PM_{2.5-10}$, indicating that SO_4^{2-}, NH_4^+, and NO_3^- mainly exist as fine particles, as also observed in a previous study (Cheng *et al.*, 2015). This source is highly related to the photochemical reactions of SO_2, NH_3, and NO*x* (Wang *et al.*, 2006; Perrone *et al.*, 2010). Therefore, stricter measures of precursor gas control are necessary to decrease $PM_{2.5}$ pollution.

The fifth factor is identified as industry and mainly includes Fe, Mn, V, Cu, Zn, Cd, Se, As, Ag, V, Ba, Pb, OC, and EC. These elements are generally associated with iron/steel or other metals used in manufacturing (Chan *et al.*, 1997; Turpin and Lim, 2001), whereas carbonaceous aerosols are also emitted from industrial sources (Zhang *et al.*, 2013b). The output of 10 kinds of nonferrous metals (e.g., Cu, Pb, and Zn) in Zhengzhou totaled 0.53 million tons in 2014 (Bureau of Statistics of Henan Province, 2015), suggesting that related industries serve as important sources of PM emission. The industry source contributed 14.6%, 11.6%, and 13.5% of $PM_{2.5}$, $PM_{2.5-10}$, and PM_{10}, respectively, implying that these species slightly but highly contribute to fine particles. This conclusion agrees with the results of chemical analysis, i.e., Zn, Pb, Cu, As, Cd, and Ag mainly exist in $PM_{2.5}$.

The sixth factor includes the unidentified sources, particularly unorganized emission sources, including biomass burning and garbage incineration. This source contributed 6.3%, 11.6%, and 10.3% of $PM_{2.5}$, $PM_{2.5-10}$, and PM_{10}, respectively.

Only CMB 8.2 (US EPA, 2004) was applied in this study to estimate source contributions to $PM_{2.5}$ owing to the lack of local chemical profiles of main sources for $PM_{2.5-10}$ and PM_{10}. According to a previous study (Samara, 2005), using source profiles entirely from literature as input data for CMB presents substantial bias in source contribution. In

our previous work (Jiang *et al.*, 2018b), dust, secondary aerosols, coal combustion, biomass burning, vehicular traffic, and industrial emission were determined as the main sources of $PM_{2.5}$ in Zhengzhou. The profiles of $PM_{2.5}$ are summarized as follows: dust and biomass profiles were established with the support by the Public Welfare Project from MEPPRC, and additional details were described by Jiang *et al.* (2018a) and Wang *et al.* (2016d), respectively; the vehicle profile was acquired from the Jingguang North Road Tunnel in Zhengzhou via a tunnel experiment and was also supported by the project. Details of this study will be reported in another paper. Secondary aerosol profiles, including those of sulfate and nitrate, were purely stoichiometric, and profiles of coal combustion and industry were acquired from previous studies (Chen *et al.*, 1994; Zheng *et al.*, 2005). Contributions of seven sources, namely, dust, biomass burning, vehicular traffic, nitrate, sulfate, coal combustion, and the industry, were calculated by CMB. According to model requirements (US EPA, 2004), R^2 (0.86), X^2 (0.43), and percentage mass (93.5%) were all in the qualified range.

Table 3 lists the CMB results of source appointment for $PM_{2.5}$. Secondary aerosols, including sulfate (18.2%) and nitrate (11.7%), are the most important sources and accounted for 29.8% of $PM_{2.5}$. Coal combustion, dust, vehicular traffic, industry, and biomass burning contributed 18.8%, 12.7%, 11.8%, 11.5%, and 8.8%, respectively, of $PM_{2.5}$. These findings were consistent with mass reconstruction and PMF results for $PM_{2.5}$, excluding that for biomass burning source. In the results of PM source apportionment by PMF, biomass burning was not identified alone. For comparison, source contributions of dust and coal combustion under CMB (12.7% and 18.8%, respectively) were similar to those under PMF (13.1% and 16.1%, respectively), whereas contributions of secondary aerosols, vehicular traffic, and industry sources under the CMB model (29.8%, 11.8%, and 11.5%, respectively) were lower than those from PMF model (35.8%, 14.1%, and 14.6%, respectively). In this study, the source profiles obtained by PMF analysis were combined with those of redundant species, i.e., the species beyond specific sources, as a potential important reason.

Back-trajectory Cluster Analysis

The back trajectories for each of the identified cluster in four seasons during the sampling period are shown in Fig. 7, and the total spatial variation percent in all the clusters was below 10%. Cluster analysis results revealed that air mass transport significantly influenced PM pollution in Zhengzhou. Air quality across the four seasons was mainly affected by air masses from different directions. Air masses from the northeast were relative constant across the four seasons and accounted for 17.2% (cluster 3 in spring) to 29.6%

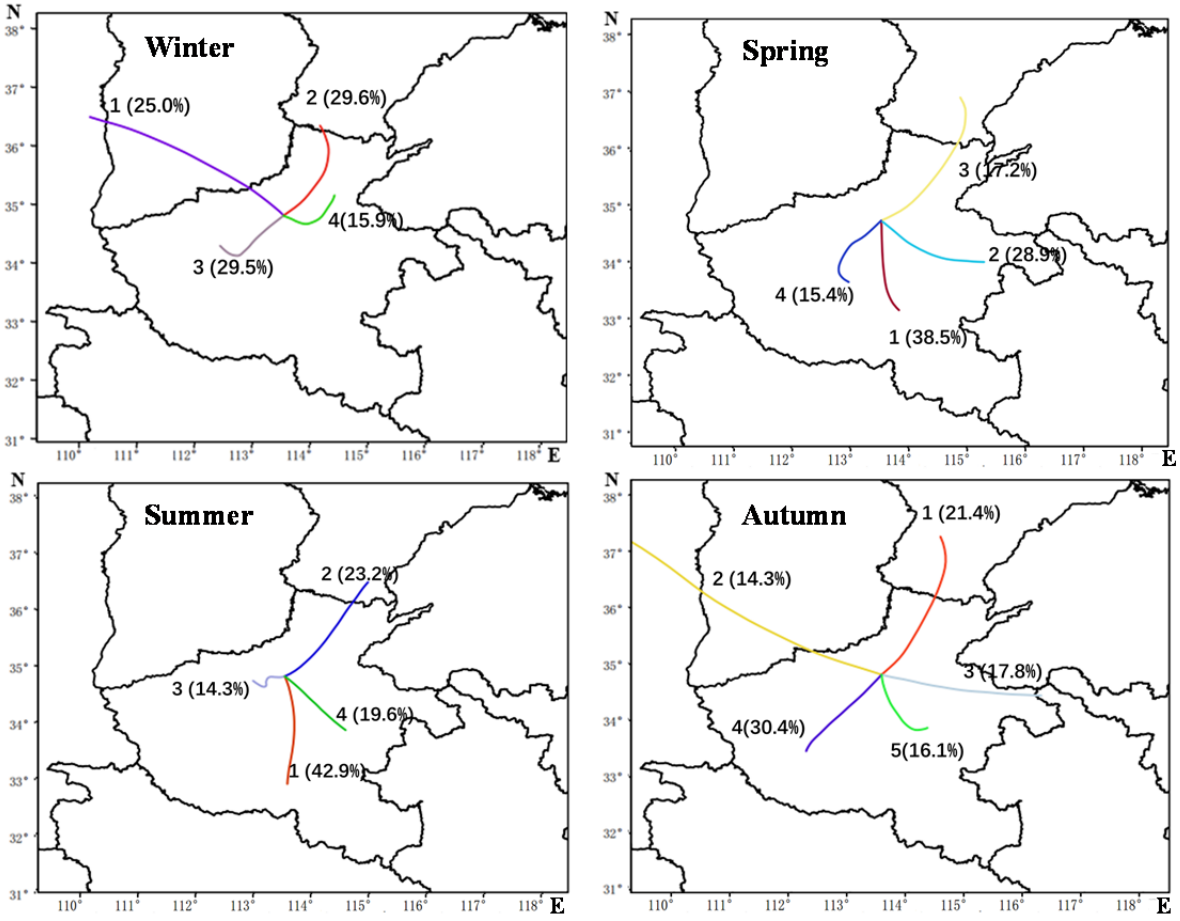

Fig. 7. Back trajectories for each of the identified cluster in four seasons during the sampling period.

(cluster 2 in winter) of all air masses. In terms of AOD, the Beijing-Tianjin-Hebei region (i.e., northeast direction) was one of the most highly deteriorated regions of aerosol pollution in China in 2014 (Fig. 1(a)). Therefore, air masses from the northeast carried a considerable amount of pollutants and probably aggravated PM pollution levels in the study area. The sustained air masses from the east accounted for 15.9% (cluster 4 in winter) to 28.9% (cluster 2 in spring). Air masses from the south, with a relatively low PM pollution (Fig. 1(a)), exhibited a more prominent effect in spring and summer than in the other two seasons and accounted for 38.5% and 42.9%, respectively, of total air masses. Notably, PM level in the study area decreased because of dilution function. Obstructed by the Taihang Mountains, air masses from the northwest direction presented much better air quality (Fig. 1(a)) and only appeared in winter (25.0%) and autumn (14.3%) under strong air circulation. However, owing to their high altitude, airflow on mountains caused no significant effects on ground wind speed in the study region (average wind speeds of 1.4 and 1.7 m s^{-1} in winter and autumn, respectively [Table 1]). Thus, air quality in winter and autumn remained poor. The highest $PM_{2.5}$ concentrations appeared with short air-mass trajectory lines, with air masses accounting for 15.9% (cluster 4 in winter; average $PM_{2.5}$: 160 μg m^{-3}), 38.5% (cluster 1 in spring; average $PM_{2.5}$: 92 μg m^{-3}), 19.6% (cluster 4 in summer; average $PM_{2.5}$: 78 μg m^{-3}), and 16.1% (cluster 5 in autumn; average $PM_{2.5}$: 122 μg m^{-3}) of total air masses in different seasons ($PM_{2.5}$ data from the national monitoring site). These results indicate the notable transport influence from the adjacent regions.

CONCLUSIONS

This study investigated the major precursors, mass levels, chemical compositions, and source apportionments of size-segregated aerosols, i.e., $PM_{2.5}$, $PM_{2.5\text{-}10}$, and PM_{10}, in Zhengzhou, an emerging megacity of east-central China. Results showed that high levels of major PM precursors, i.e., NO_2 and SO_2, play an important role in serious PM pollution. The average annual concentrations of $PM_{2.5}$ and PM_{10} were 187 and 281 μg m^{-3}, respectively, which are much higher than those of the Chinese NAAQS. Concentrations of the size-segregated aerosols exhibited remarkable seasonal characteristics, with the highest average concentrations in winter and the lowest values in summer.

The results of the chemical analysis indicated that SIAs were the major ions in PM and mainly existed in the fine particles: SIAs accounted for 36%, 10%, and 27% of $PM_{2.5}$, $PM_{2.5\text{-}10}$, and PM_{10}, respectively. Spearman correlation coefficient analysis revealed biomass burning and dust as important sources of PM. The annual concentrations of As (0.029 μg m^{-3}) and Cd (0.010 μg m^{-3}) in the PM_{10} remarkably exceeded those of the Chinese NAAQS and implied a relatively high health risk. After comparing the elemental compositions of the size-segregated aerosols, we found that Zn, Pb, Cu, As, Sn, Cd, Sb, Tl, and Ag mainly existed in the $PM_{2.5}$. By contrast, Al, Fe, Mg, Ti, Ba, and Sr were relatively comparable in the $PM_{2.5}$ and the $PM_{2.5\text{-}10}$. Results of mass reconstruction of the size-segregated aerosols revealed that CM was more abundant in coarse particles than in fine particles but SIAs were primarily present in $PM_{2.5}$.

The PMF results indicated that source contribution characteristics differed among the size-segregated aerosols. Overall, dust, vehicular traffic, coal combustion, secondary aerosols, and industry served as the main pollution sources, accounting for 13.1%, 14.1%, 16.1%, 35.8%, and 14.6% in $PM_{2.5}$; 25.1%, 20.8%, 21.8%, 10.5%, and 11.6% in $PM_{2.5\text{-}10}$; and 19.8%, 15.8%, 18.5%, 22.5%, and 13.5% in PM_{10}, respectively. Dust sources played an important role in coarse particles, indicating that appropriate dust control measures more effectively decrease PM_{10} levels than $PM_{2.5}$ levels. However, secondary aerosol sources provided the highest contribution to $PM_{2.5}$, suggesting that controlling precursor gases (i.e., SO_2, NO_x, NH_3, and VOCs) can be more effective in reducing fine particles than coarse ones. The CMB findings agreed with the PMF results for $PM_{2.5}$. For comparison, the contributions of secondary aerosol, vehicular traffic, and industrial sources were lower in the CMB model than the PMF model.

Cluster analysis showed that air quality across the four seasons was mainly affected by air masses from the northeast (17.2%–29.6%) and the east (15.9%–28.9%), indicating the significant influence of transport from the Beijing-Tianjin-Hebei region and the adjacent regions, respectively. Air masses from the south exhibited an important dilution function.

ACKNOWLEDGMENT

The study was supported by the Public Welfare Project from the Ministry of Environmental Protection of the People's Republic of China (Grant No. 201409010) and the Central Leading Local Development of Science and Technology Project in China (Grant No. HN 2016–149). Authors would like to appreciate those assisting in analysis: Jia Wang, Panru Kang, and Leishi Zhang.

SUPPLEMENTARY MATERIAL

Supplementary data associated with this article can be found in the online version at http://www.aaqr.org.

REFERENCES

Amato, F., Alastuey, A., Karanasiou, A., Lucarelli, F., Nava, S., Calzolai, G., Severi, M., Becagli, S., Gianelle, V.L., Colombi, C., Alves, C., Custódio, D., Nunes, T., Cerqueira, M., Pio, C., Eleftheriadis, E., Diapouli, E., Reche, C., Minguillón, M.C., Manousakas, M.I., Maggos, T., Vratolis, S., Harrison, R.M. and Querol, X. (2016). AIRUSE-LIFE+: A harmonized PM speciation and source apportionment in five southern European cities. *Atmos. Chem. Phys.* 16: 23989–24039.

Bao, Z., Feng, Y.C., Jiao, L., Hong, S.M. and Liu, W.G. (2010). Characterization and source apportionment of $PM_{2.5}$ and PM_{10} in Hangzhou. *Environ. Monit. China* 26: 44–48.

Bhangare, R.C., Ajmal, P.Y., Sahu, S.K., Pandit, G.G. and Puranik, V.D. (2011). Distribution of trace elements in coal and combustion residues from five thermal power plants in India. *Int. J. Coal Geol.* 86: 349–356.

Bozlaker, A., Spada, N.J., Fraser, M.P. and Chellam, S. (2013). Elemental characterization of $PM_{2.5}$ and PM_{10} emitted from light duty vehicles in the Washburn Tunnel of Houston, Texas: Release of rhodium, palladium, and platinum. *Environ. Sci. Technol.* 48: 54–62.

Brown, S.G., Eberly, S., Paatero, P. and Norris, G.A. (2015). Methods for estimating uncertainty in PMF solutions: Examples with ambient air and water quality data and guidance on reporting PMF results. *Sci. Total Environ.* 518: 626–635.

Bureau of Statistics of Henan Province (2011). *Henan statistical yearbook 2011*, China Statistics Press, Beijing (in Chinese).

Bureau of Statistics of Henan Province (2015). *Henan statistical yearbook 2015*, China Statistics Press, Beijing (in Chinese).

Cesari, D., Donateo, A., Conte, M. and Contini, D. (2016a). Inter-comparison of source apportionment of PM_{10}, using PMF and CMB in three sites nearby an industrial area in central Italy. *Atmos. Res.* 182: 282–293.

Cesari, D., Donateo, A., Conte, M., Merico, E., Giangreco, A., Giangreco, F. and Contini, D. (2016b). An inter-comparison of $PM_{2.5}$, at urban and urban background sites: chemical characterization and source apportionment. *Atmos. Res.* 174–175: 106–119.

Chameides, W.L., Yu, H., Liu, S.C., Bergin, M., Zhou, X., Mearns, L., Wang, G., Kiang, C.S., Saylor, R.D., Luo, C. and Huang, Y. (1999). Case study of the effects of atmospheric aerosols and regional haze on agriculture: an opportunity to enhance crop yields in China through emission controls? *Proc. Natl. Acad. Sci. U.S.A.* 96: 13626–13633.

Chan, Y.C., Simpson, R.W., Mctainsh, G.H., Vowles, P.D., Cohen, D.D. and Bailey, G.M. (1997). Characterisation of chemical species in $PM_{2.5}$ and PM_{10} aerosols in Brisbane, Australia. *Atmos. Environ.* 31: 3773–3785.

Charlesworth, S., Miguel, E.D. and Ordóñez, A. (2011). A review of the distribution of particulate trace elements in urban terrestrial environments and its application to considerations of risk. *Environ. Geochem. Health* 33: 103–123.

Charlson, R.J., Schwartz, S.E., Hales, J.M., Cess, R.D., Coakley, J.A., Hansen, J.E. and Hofmann, D.J. (1992). Climate forcing by anthropogenic aerosols. *Science* 255: 423–430.

Chen, L.W., Chow, J.C., Doddridge, B.G., Dickerson, R.R., Ryan, W.F. and Mueller, P.K. (2003). Analysis of a summertime $PM_{2.5}$ and haze episode in the mid-Atlantic region. *J. Air Waste Manage. Assoc.* 53: 946–956.

Chen, Z., Ge, S. and Zhang, J. (1994). Measurement and analysis for atmospheric aerosol particulates in Beijing. *Res. Environ. Sci.* 7: 1–9.

Cheng, Y., Lee, S.C., Ho, K.F., Chow, J.C., Watson, J.G., Louie, P.K.K., Cao, J.J. and Hai, X. (2010). Chemically-speciated on-road $PM_{2.5}$ motor vehicle emission factors in Hong Kong. *Sci. Total Environ.* 408: 1621–1627.

Cheng, Y., Lee, S.C., Gu, Z.L., Ho, K.F., Zhang, Y.W., Huang, Y., Chow, J.C., Watson, J.G., Gao, J.J. and Zhang, R.J. (2015). $PM_{2.5}$ and $PM_{10\text{-}2.5}$ chemical composition and source apportionment near a Hong Kong roadway. *Particuology* 18: 96–104.

Chow, J.C., Watson, J.G., Crow, D., Lowenthal, D.H. and Merrifield, T. (2001). Comparison of IMPROVE and NIOSH carbon measurement. *Aerosol Sci. Technol.* 34: 23–34.

Chow, J.C., Lowenthal, D.H., Chen, L.W.A., Wang, X. and Watson, J.G. (2015). Mass reconstruction methods for $PM_{2.5}$: A review. *Air Qual. Atmos. Health* 8: 243–263.

Contini, D., Cesari, D., Conte, M. and Donateo, A. (2016). Application of PMF and CMB receptor models for the evaluation of the contribution of a large coal-fired power plant to PM_{10} concentrations. *Sci. Total Environ.* 560–561: 131–140.

Economist Intelligence Unit (2012). Supersized cities China's 13 megalopolises. https://www.eiu.com/public/topical_report.aspx?campaignid=Megalopolis2012

Eldred, R.A., Cahill, T.A. and Flocchini, R.G. (1997). Composition of $PM_{2.5}$ and PM_{10} aerosols in the IMPROVE network. *J. Air Waste Manage. Assoc.* 47: 194–203.

Garg, B.D., Cadle, S.H., Mulawa, P.A., Groblicki, P.J., Laroo, C. and Parr, G.A. (2000). Brake wear particulate matter emissions. *Environ. Sci. Technol.* 34: 4463–4469.

Geng, N.B., Wang, J., Xu, Y.F., Zhang, W.D., Chen, C. and Zhang, R.Q. (2013). $PM_{2.5}$ in an industrial district of Zhengzhou, China: Chemical composition and source apportionment. *Particuology* 11: 99–109.

Gianini, M.F.D., Piot, C., Herich, H., Besombes, J.L., Jaffrezo, J.L. and Hueglin, C. (2013). Source apportionment of PM_{10}, organic carbon and elemental carbon at Swiss sites: An intercomparison of different approaches. *Sci. Total Environ.* 454–455: 99–108.

Guo, Y.M., Tong, S.L., Zhang, Y.S., Barnett, A.G., Jia, Y.P. and Pan, X.C. (2010). The relationship between particulate air pollution and emergency hospital visits for hypertension in Beijing, China. *Sci. Total Environ.* 408: 4446–4450.

Hadley, O.L. (2017). Background $PM_{2.5}$ source apportionment in the remote Northwestern United States. *Atmos. Environ.* 167: 298–308.

Hand, J.L., Copeland, S.A., McDade, C.E., Day, D.E., Moore, J.C.T., Dillner, A.M., Pitchford, M.L., Indresand, H., Schichtel, B.A., Malm, W.C. and Watson, J.G. (2011). *Spatial and seasonal patterns and temporal variability of haze and its constituents in the United States, IMPROVE Report V*. Cooperative Institute for Research in the Atmosphere, Fort Collins.

Jang, E., Alam, M.S. and Harrison, R.M. (2013). Source apportionment of polycyclic aromatic hydrocarbons in urban air using positive matrix factorization and spatial distribution analysis. *Atmos. Environ.* 79: 271–285.

Jiang, N., Guo, Y., Wang, Q., Kang, P.R., Zhang, R.Q. and Tang, X.Y. (2017). Chemical composition characteristics of $PM_{2.5}$ in three cities in Henan, central China. *Aerosol Air Qual. Res*. 17: 2367–2380.

Jiang, N., Dong, Z., Xu, Y.Q., Yu, F., Yin, S.S., Zhang, R.Q. and Tang, X.Y. (2018a). Characterization of PM_{10} and $PM_{2.5}$ source profiles for fugitive dust in Zhengzhou, China. *Aerosol Air Qual. Res.* 18: 314–329.

Jiang, N., Li, Q., Su, F.C., Wang, Q., Yu, X., Kang, P.R., Zhang, R.Q. and Tang, X.Y. (2018b). Chemical characteristics and source apportionment of $PM_{2.5}$, between heavily polluted days and other days in Zhengzhou, China. *J. Environ. Sci.* 66: 188–198.

Jiang, N., Yin, S.S., Guo, Y., Li, J.Y., Kang, P.R., Zhang, R.Q. and Tang, X.Y. (2018c). Characteristics of mass concentration, chemical composition, source apportionment of $PM_{2.5}$ and PM_{10} and health risk assessment in the emerging megacity in China. *Atmos. Pollut. Res.* 9: 309–321.

Kang, C.M., Lee, H.S., Kang, B.W., Lee, S.K. and Sunwoo, Y. (2004). Chemical characteristics of acidic gas pollutants and $PM_{2.5}$ species during hazy episodes in Seoul, South Korea. *Atmos. Environ.* 38: 4749–4760.

Kim, E., Larson, T.V., Hopke, P.K., Slaughter, C., Sheppard, L.E. and Claiborn, C. (2003). Source identification of $PM_{2.5}$ in an arid northwest U.S. city by positive matrix factorization. *Atmos. Res.* 66: 291–305.

Kong, S.F., Han, B., Bai, Z.P., Chen, L., Shi, J.W. and Xu, Z. (2010). Receptor modeling of $PM_{2.5}$, PM_{10} and TSP in different seasons and long-range transport analysis at a coastal site of Tianjin, China. *Sci. Total Environ.* 408: 4681–4694.

Krotkov, N.A., Mclinden, C.A., Li, C., Lamsal, L.N., Celarier, E.A., Marchenko, S.V., Swartz, W.H., Bucsela, E.J., Joiner, J., Duncan, B.N., Boersma, K.F., Veefkind, J.P., Levelt, P.F., Fioletov, V.E., Dickerson, R.R., He, H., Lu, Z. and Streets, D.G. (2016). Aura OMI observations of regional SO_2 and NO_2 pollution changes from 2005 to 2014. *Atmos. Chem. Phys.* 16: 4605–4629.

Lasun, T.O., Oyediran, K.O., Felix, S.O. and Philip, K.H. (2016). Source identification and apportionment of $PM_{2.5}$ and $PM_{2.5\text{-}10}$ in iron and steel scrap smelting factory environment using PMF, PCFA and UNMIX receptor models. *Environ. Monit. Assess.* 188: 574.

Li, H., Wang, Q., Yang, M., Li, F., Wang, J., Sun, Y., Wang, C., Wu, H. and Qian, X. (2016). Chemical characterization and source apportionment of $PM_{2.5}$ aerosols in a megacity of Southeast China. *Atmos. Res.* 181: 288–299.

Lin, Y.C., Tsai, C.J., Wu, Y.C., Zhang, R., Chi, K.H., Huang, Y.T., Lin, S.H. and Hsu, S.C. (2014). Characteristics of trace metals in traffic-derived particles in Hsuehshan Tunnel, Taiwan: Size distribution, fingerprinting metal ratio, and emission factor. *Atmos. Chem. Phys.* 14: 4117–4130.

Liu, A., Liu, L., Li, D. and Guan, Y. (2015). Characterizing heavy metal build-up on urban road surfaces: Implication for stormwater reuse. *Sci. Total Environ.* 515–516: 20–29.

Liu, B.S., Song, N., Dai, Q.L., Mei, R.B., Sui, B.H., Bi, X.H. and Feng, Y.C. (2016). Chemical composition and source apportionment of ambient $PM_{2.5}$ during the non-heating period in Taian, China. *Atmos. Res.* 170: 23–33.

Long, S.L., Zeng, J.R., Li, Y., Bao, L.M., Cao, L.L., Liu, K., Xu, L., Lin, J., Liu, W., Wang, G.H., Yao, J., Ma, C.Y. and Zhao, Y.D. (2014). Characteristics of secondary inorganic aerosol and sulfate species in size-fractionated aerosol particles in Shanghai. *J. Environ. Sci.* 26: 1040–1051.

Lough, G.C., Schauer, J.J., Park, J.S., Shafer, M.M., Deminter, J.T., Weinstein, J.P. (2005). Emissions of metals associated with motor vehicle roadways. *Environ. Sci. Technol.* 39: 826–836.

Luo, Y.X., Zheng, X.B., Zhao, T.L. and Chen, J. (2014). A climatology of aerosol optical depth over China from recent 10 years of MODIS remote sensing data. *Int. J. Climatol.* 34: 863–870.

Malm, W.C., Sisler, J.F., Huffman, D., Eldred, R.A. and Cahill, T.A. (1994). Spatial and seasonal trends in particle concentration and optical extinction in the United States. *J. Geophys. Res.* 99: 1347–1370.

Manousakas, M., Diapouli, E., Papaefthymiou, H., Migliori, A., Karydas, A.G., Padilla-Alvarez, R., Bogovac, M., Kaiser, R.B., Jaksic, M., Bogdanovic-Radovic, I. and Eleftheriadisb, K. (2015). Source apportionment by PMF on elemental concentrations obtained by PIXE analysis of PM_{10} samples collected at the vicinity of lignite power plants and mines in Megalopolis, Greece. *Nucl. Instrum. Methods Phys. Res. B* 349: 114–124.

Martuzevicius, D., Kliucininkas, L., Prasauskas, T., Krugly, E., Kauneliene, V. and Strandberg, B. (2011). Resuspension of particulate matter and PAHs from street dust. *Atmos. Environ.* 45: 310–317.

MEPPRC (2015). Report on the state of the environment in China. http://english.mep.gov.cn/Resources/Reports/soe/soe2011/201606/P020160601592064474593.pdf

National Bureau of Statistics of China (2015). *China statistical yearbook 2015.* China Statistics Press, Beijing (in Chinese).

Paatero, P. and Tapper, U. (1994). Positive matrix factorization: A non-negative factor model with optimal utilization of error estimates of data values. *Environmetrics* 5: 111–126.

Peng, G.L., Wang, X.M., Wu, Z.Y., Wang, Z.M., Yang, L.L., Zhong, L.J. and Chen, D.H. (2011). Characteristics of particulate matter pollution in the Pearl River Delta region, China: An observational-based analysis of two monitoring sites. *J. Environ. Monit.* 13: 1927–1934.

Perrone, M.G., Gualtieri, M., Ferrero, L., Porto, C.L., Udisti, R., Bolzacchini, E. and Camatini, M. (2010). Seasonal variations in chemical composition and in vitro biological effects of fine PM from Milan. *Chemosphere* 78: 1368–1377.

Querol, X., Alastuey, A., Ruiz, C.R., Arti´nano, B., Hansson, H.C., Harrison, R.M., Buringh, E., Brink, H.M., Lutz, M., Bruckmann, P., Straehl, P. and Schneider, J. (2004). Speciation and origin of PM_{10} and $PM_{2.5}$ in selected European cities. *Atmos. Environ.* 38: 6547–6555.

Ramanathan, V., Crutzen, P. J., Lelieveld, J., Mitra, A. P., Althausen, D., Anderson, J., Andreae, M.O., Cantrell, W., Cass, G.R., Chung, C.E., Clarke, A.D., Coakley, J.A., Collins, W.D., Conant, W.C., Dulac, F., Heintzenberg, J., Heymsfield, A. J., Holben, B., Howell, S., Hudson, J.,

Jayaraman, A., Kiehl, J.T., Krishnamurti, T.N., Lubin, D., McFarquhar, G., Novakov, T., Ogren, J.A., Podgorny, I.A., Prather, K., Priestley, K., Prospero, J.M., Quinn, P.K., Rajeev, K., Rasch, P., Rupert, S., Sadourny, R., Satheesh, S.K., Shaw, G.E., Sheridan, P., and Valero, F.P.J. (2001). Indian ocean experiment: An integrated analysis of the climate forcing and effects of the great indo-asian haze. *J. Geophys. Res.* 106: 28371–28398.

Samara, C. (2005). Chemical mass balance source apportionment of TSP in a ligniteburning area of Western Macedonia, Greece. *Atmos. Environ.* 39: 6430–6443.

Shi, G.L., Liu, G.R., Peng, X., Wang, Y.N., Tian, Y.Z., Wang, W. and Feng, Y.C. (2014). A comparison of multiple combined models for source apportionment, including the PCA/MLR-CMB, Unmix-CMB and PMF-CMB models. *Aerosol Air Qual. Res.* 14: 2040–2050.

Silva, P.J., Liu, D.., Noble, C.A. and Prather, K.A. (1999). Size and chemical characterization of individual particles resulting from biomass burning of local southern California species. *Environ. Sci. Technol.* 33: 3068–3076.

Simon, H., Bhave, P.V., Swall, J.L., Frank, N.H. and Malm, W.C. (2011). Determining the spatial and seasonal variability in OM/OC ratios across the US using multiple regression. *Atmos. Chem. Phys.* 11: 2933–2949.

Sun, Y.L., Zhuang, G.S., Tang, A.H., Wang, Y. and An, Z.S. 2006. Chemical characteristics of $PM_{2.5}$ and PM_{10} in haze-fog episodes in Beijing. *Environ. Sci. Technol.* 40: 3148–3155.

Tao, J., Zhang, L.M., Engling, G., Zhang, R.R., Yang, Y.H., Cao, J.J., Zhu, C.S., Wang, Q.Y. and Luo, L. (2013). Chemical composition of $PM_{2.5}$ in an urban environment in Chengdu, China: importance of springtime dust storms and biomass burning. *Atmos. Res.* 122: 270–283.

Tao, M., Chen, L., Wang, Z., Wang, J., Tao, J. and Wang, X. (2016). Did the widespread haze pollution over china increase during the last decade? A satellite view from space. *Environ. Res. Lett.* 11: 054019.

Tauler, R., Viana, M., Querol, X., Alastuey, A., Flight, R.M., Wentzell, P.D. and Hopke, P.K. (2009). Comparison of the results obtained by four receptor modelling methods in aerosol source apportionment studies. *Atmos. Environ.* 43: 3989–3997.

Taylor, S.R. and Mclennan, S.M. (1995). The geochemical evolution of the continental crust. *Rev. Geophys.* 33: 293–301.

Tian, Y.Z., Shi, G.L., Huang-fu, Y.Q., Song, D.L., Liu, J.Y., Zhou, L.D. and Feng, Y.C. (2016). Seasonal and regional variations of source contributions for PM_{10} and $PM_{2.5}$ in urban environment. *Sci. Total Environ.* 557–558: 697-704.

Turpin, B.J. and Lim, H.J. (2001). Species contributions to $PM_{2.5}$ mass concentrations: revisiting common assumptions for estimating organic mass. *Aerosol Sci. Technol.* 35: 602–610.

US EPA (2004). EPA-CMB8.2 user manual. United States Environmental Protection Agency, Washington, DC. https://www3.epa.gov/ttn/scram/models/receptor/EPA-CMB82Manual.pdf

US EPA (2014). Positive matrix factorization (PMF) 5.0 fundamentals and user guide. Office of Research and Development, Washington, DC. https://www.epa.gov/sites/production/files/2015-02/documents/pmf_5.0_user_guide.pdf

US EPA (2016). Definition and Procedure for the Determination of the Method Detection Limit, Revision 2. Office of Science and Technology, Washington, DC. https://www.epa.gov/sites/production/files/2016-12/documents/mdl-procedure_rev2_12-13-2016.pdf

Viana, M., Querol, X., Alastuey, A., Gil, J.I. and Menéndez, M. (2006). Identification of PM sources by principal component analysis (PCA) coupled with wind direction data. *Chemosphere* 65: 2411–2418.

Wang, H.L., Qiao, L.P., Lou, S.R., Zhou, M., Ding, A.J., Huang, H.Y., Chen, J.M., Wang, Q., Tao, S.K., Chen, C.H., Li, L. and Huang, C. (2016a). Chemical composition of $PM_{2.5}$ and meteorological impact among three years in urban Shanghai, China. *J. Cleaner Prod.* 112: 1302–1311.

Wang, J., Hu, Z.M., Chen, Y.Y., Chen, Z.L. and Xu, S.Y. (2013). Contamination characteristics and possible sources of PM_{10} and $PM_{2.5}$ in different functional areas of Shanghai, China. *Atmos. Environ.* 68: 221–229.

Wang, J., Li, X., Jiang, N., Zhang, W., Zhang, R.Q. and Tang, X. (2015). Long term observations of $PM_{2.5}$-associated PAHs: Comparisons between normal and episode days. *Atmos. Environ.* 104: 228–236.

Wang, J., Li, X., Zhang, W. K., Jiang, N., Zhang, R.Q. and Tang, X.Y. (2016b). Secondary $PM_{2.5}$ in Zhengzhou, China: Chemical species based on three years of observations. *Aerosol Air Qual. Res.* 16: 91–104.

Wang, J., Zhang, Y.F., Feng, Y.C., Zheng, X.J., Jiao, L., Hong, S.M., Zhu, T., Ding, J. and Zhang, Q. (2016c). Characterization and source apportionment of aerosol light extinction with a coupled model of CMB-IMPROVE in Hangzhou, Yangtze River Delta of China. *Atmos. Res.* 178–179: 570–579.

Wang, K., Dickinson, R.E., Su, L. and Trenberth, K.E. (2012). Contrasting trends of mass and optical properties of aerosols over the northern hemisphere from 1992 to 2011. *Atmos. Chem. Phys.* 12: 17913-17941.

Wang, Q., Jiang, N., Yin, S., Li, X., Yu, F., Guo, Y. and Zhang R. (2017). Carbonaceous species in $PM_{2.5}$, and PM_{10}, in urban area of Zhengzhou in China: Seasonal variations and source apportionment. *Atmos. Res.* 191: 1–11.

Wang, X., Bi, X., Sheng, G. and Fu, J. (2006). Chemical composition and sources of PM_{10} and $PM_{2.5}$ aerosols in Guangzhou, China. *Environ. Monit. Assess.* 119: 425–439.

Wang, Y., Hu, M., Wang, Y., Qin, Y., Chen, H., Zeng, L., Lei, J., Huang, X., He, L., Zhang, R. and Wu, Z. (2016d). Characterization and influence factors of $PM_{2.5}$ emitted from crop straw burning. *Acta Chim. Sinica* 74: 356–362.

Wang, Y.Q. (2014). MeteoInfo: GIS software for meteorological data visualization and analysis. *Meteorol. Appl.* 21: 360–368.

Winchester, J.W., Ferek, R.J., Lawson, D.R., Pilotte, J.O.,

Thiemens, M.H. and Wangen, L.E. (1979). Comparison of aerosol sulfur and crustal element concentrations in particle size fractions from continental U. S. locations. *Water Air Soil Pollut.* 12: 431–440.

Xie, Y.L., Hopke, P.K., Paatero, P., Barrie, L.A. and Li, S.M. (1999). Identification of source nature and seasonal variations of arctic aerosol by positive matrix factorization. *J. Atmos. Sci.* 56: 249–260.

Yatkin, S. and Bayram, A. (2008). Source apportionment of PM_{10}, and $PM_{2.5}$, using positive matrix factorization and chemical mass balance in izmir, turkey. *Sci. Total Environ.* 390: 109–123.

Zhang, F.W., Xu, L.L., Chen, J.S., Chen, X.Q., Niu, Z.C., Lei, T., Li, C.M. and Zhao, J.P. (2013a). Chemical characteristics of $PM_{2.5}$ during haze episodes in the urban of Fuzhou, China. *Particuology* 11: 264–272.

Zhang, R., Jing, J., Tao, J., Hsu, S.C., Wang, G., Cao, J., Lee, C.S.L., Zhu, L., Chen, Z., Zhao, Y. and Shen, Z. (2013b). Chemical characterization and source apportionment of $PM_{2.5}$ in Beijing: Seasonal perspective. *Atmos. Chem. Phys.* 13: 7053–7074.

Zheng, M., Salmon, L.G., Schauer, J.J., Zeng, L., Kiang, C.S., Zhang, Y.H. and Cass G.R. (2005). Seasonal trends in $PM_{2.5}$ source contributions in Beijing, China. *Atmos. Environ.* 39: 3967–3976.

Zheng, G.J., Duan, F.K., Su,H., Ma, Y.L., Cheng, Y., Zheng, B., Zhang, Q., Huang, T., Kimoto, T., Chang, D., Pöschl, U., Cheng, Y.F. and He, K.B. (2015). Exploring the severe winter haze in Beijing: The impact of synoptic weather, regional transport and heterogeneous reactions. *Atmos. Chem. Phys.* 15: 2969–2983.

Zhou, R., Xing, J.Y., Xing, L.T., Wang, X.Y., Feng, X.X., Ji, D.S. and Wang, Y.S. (2011). Variation of air pollution in new Tangshan industrial area during winter heating period. *Environ.Sci.* 32: 1874–1880 (in Chinese).

Received for review, October 26, 2017
Revised, February 22, 2018
Accepted, April 23, 2018